Visible-light-driven Photocatalytic Properties of Electrospun Bismuth Tungstate/PAN Composite Nanofiber Membrane

XINHUA LIU[a*], HONGZHANG LI[b], ZHI LIU[a*], YINCHUN FANG[a] AND CUIE WANG[a]

[a]*School of Textile and Garment, Anhui Polytechnic University, Wuhu, 241000, China*
[b]*Jiangmen Polytechnic, Jiangmen 529030, China*

ABSTRACT

Bismuth Tungstate has been widely used in catalytic degradation of pollutants. However, the low specific surface area make it difficult to use. Herein, bismuth/tungstate/polyacrylonitrile (PAN) nanofiber was prepared by electrospinning. After oxidation treatment, the bismuth tungstate/ PAN composite nanofiber membrane showed photo catalytic activity. The photocatalytic property of resulting membrane was evaluated by the photodegradation of methylene blue. The results showed that the photodegradation rate reached to 95.53% after 4.5h. The photodegradation rate of the membrane still preserved 83.88% after 8 times reuse, indicating its reusability. Thus, the visible-light-catalyst has potential application in sewage treatment.

KEYWORDS: *Bismuth tungstate, PAN, Photocatalysis, Visible light, Water treatment.*

1. INTRODUCTION

Photocatalysis technology uses sunlight as the source energy to catalyze chemical reactions. In the photocatalysis process, photocatalysts can absorb photons to produce a variety of active free radicals which can effectively degrade varieties of toxic chemicals [1,2].

Perovskite bismuth tungstate (Bi_2WO_6) was found to possess excellent photocatalytic properties on organic pollutants under visible light irradiation [3-5]. On account of the molecular and electronic versatility, reactivity, stability, etc., Bi_2WO_6 is a kind of promising photocatalyst. In 1999, Kudo and Hijii [6] firstly reported that Bi_2WO_6 was active for the oxygen evolution reaction under visible light irradiation with the Aurivillius structure and a 2.8 eV band gap. Afterwards, Bi_2WO_6 drew great attention as a new photocatalyst. Many methods

J. Polym. Mater. Vol. **35,** No. 3, 2018, 295-304

Correspondence author e-mail: Liuxinhua66@163.com; Liuzhi@ahpu.edu.cn
DOI : https://doi.org/10.32381/JPM.2018.35.03.4

emerged to construct the promising photocatalyst. Dai et al. [7] demonstrated a facile hydrothermal route for controllable synthesis of novel Bi_2WO_6 hierarchical hollow spheres. At the research of Zhang [8], Bi_2WO_6 was synthesized by water, methanol and ethylene glycol assisted solvothermal method. Xu et al.[9] successfully synthesized Bi_2WO_6 nano-crystals with the average size of 12 nm by a simple solvothermal method at 180 °C for 2 h. Hori et al. [10] studied the formation mechanism, structural characteristics and photocatalytic activities of hierarchical-structured bismuth-tungstate particles. With the research deepening, researchers realized that the Bi_2WO_6 photocatalyst prepared demandingly and costly, hindering the application in the practical industry. Therefore, how to optimize the technology and reduce the cost for preparing Bi_2WO_6 photocatalyst is under urgent demand.

Electrospinning is an inexpensive and versatile technique to fabricate nanofibers from a rich variety of materials [11,12]. With the high specific surface area, internal connection of pores, controllable fiber diameter and thickness, electrospun nanofiber membrane has been widely used in filter materials [13], bioengineering [14], reinforced composites [15], photocatalysis [16], etc. Electrospun nanofiber membrane, as the catalyst matrix, facilitates the dispersion and attachment of the photocatalyst and can provide more reaction sites. In our previous work [17], Bismuth Tungstate/Acrylic composite fibers were fabricated by wet-spinning process. The resulting fiber showed good photocatalytic performance while was limited by the poor reusability.

Herein, electrospun bismuth tungstate/PAN composite nanofiber membrane with visible-light-driven property was obtained after oxidation treatment. Subsequently, the resulting membrane was characterized by SEM, FTIR and XRD. Meanwhile, the photocatalytic and reusable properties were evaluated by the photodegradation of methylene blue. Gratifyingly, the results showed that the bismuth tungstate/PAN composite membrane has great visible-light photocatalytic properties and reusability.

2. EXPERIMENTAL

2.1 Materials

Polyacrylonitrile (PAN, *Mw*=10^5g/mol, the proportion of acrylonitrile, methacrylate and itaconic acid were 93.0 wt.%, 5.3 wt.% and 1.7 wt.% respectively) was purchased from Courtaulds Co. UK. N, N-Dimethylformamide (DMF), Bismuth nitrate pentahydrate ($Bi(NO_3)_3.5H_2O$), Tungstic acid sodium salt dehydrate (Na_2WO_4) were obtained from China pharmaceutical group chemical reagent co. LTD. All chemicals were of analytical grade and used without further purification.

2.2. Sample preparation

Preparation of polymeric precursor solution 20mL DMF was added to a 50mL erlenmeyer flask, and then added 2.06mmol bismuth nitrate pentahydrate. Subsequently, the solution above was treated by ultrasonic dispersion for 1h. Then, 1.03mmol sodium tungstate was added into the solution, and treated by ultrasonic dispersion for 1h. The resulting solution was uniform milky-white solution. 2g acrylic fiber was added to the solution which was dissolved by magnetic stirring for 12 hours to obtain the precursor solution.

Fabrication of bismuthtungstate/ PAN composite nanofiber by electrospinning Electrospinning experiments were carried out at room temperature in fume hood under horizontal configuration at the relative humidity of 50%. The prepared precursor

solution was doped into a metal needle syringe (0.7mm in internal diameter). The optimized spinning parameter was as follows: voltage 22kV, flow rate 0.2mL/h, tip-to-collection distance 15cm. The electrospinning experiment was carried out for 12 hours, thus a membrane with certain thickness was fabricated.

Thermal induced bismuth tungstate/PAN composite nanofiber membrane The as-prepared membrane was dried in an electro-thermal drying oven at 35°C for 12h, after which, the oven was heated up to a specified temperature (*T*) at a certain rate (*v)* and kept the *T* invariant for some time (*t*). Thus, bismuth tungstate/acrylic composite nanofiber membrane was obtained after thermal modification. The three parameters *T*, *v* and *t* were studied and optimized in the present work.

2.3. Measurements and characterizations

The morphologies of as-prepared nanofiber and oxidized nanofiber were observed using a scanning electron microscopy (SEM, Hitachi S-4800, Tokyo, Japan) at 20°C, 60% RH. Samples were sputter coated with gold layer prior to imaging. The diameters of nanofibers were calculated by measuring at least 100 nanofibers at random using Image *J* software. The average diameter $\bar{x}$ was calculated and the variable coefficient *C* was used to evaluate the dispersion of the diameters. The formula was as follows:

$$C = \frac{S}{x} \times 100\%$$

Where $\bar{x}$ is the average diameter, the *S* is the standard deviation.

The UV-vis spectrum of the resulting materials was characterized by ultraviolet and visible spectrophotometer (UV2450/2550, Shimadzu). After then, we obtained the band gap of bismuth tungstate 2.66 eV using the tangent method [18,19]. The structures of as-prepared and oxidized membrane were measured by Fourier transform infrared spectroscopy (FTIR) on IRPrestige-21 (Shimadzu Company, Tokyo). X-ray Diffraction (XW series, Bruker, Germany) was used to analysis the crystal properties of the as-prepared and oxidized membrane.

2.4. Photocatalytic activity evaluation

Maximum absorption wavelength of the methylene blue

The absorption maxima of methylene blue was obtained at 665 nm. So 665 nm was used as the analysis wavelength in the photocatalysis test.

Photocatalysis test

500W Xenon Light Source was used to simulate the sun light. Infrared filter (λ > 780nm) and ultra violet filter (λ < 420nm) were arranged around the reactor.

0.1g catalyst was added to 50ml methylene blue solution (concentration of 10 mg/L). Then the resultant solution was put in the dark room for 30 min to reach adsorption equilibrium. The degradation rate was calculated as follows:

$$D = \frac{A_0 - A_t}{A_0} \times 100\%$$

A_0 -Initial absorbance, A_t -Absorbance at time 1 sec.

3. RESULT AND DISCUSSION

3.1. Morphology of as-prepared and oxidized nanofiber

The morphology of as-prepared and oxidized nanofiber was shown in Fig. 1. The average diameter of nanofiber was 93nm with the variable coefficient 26.32%. Compared with the as-prepared nanofiber, the diameter of oxidized nanofiber increased to 113nm and showed arch structure on the fiber surface. The oxidized nanofiber becomes rough. Under the oxidation treatment, the cyclization reaction happened on the acrylic fibers which favors to the membrane strength to a certain extent.

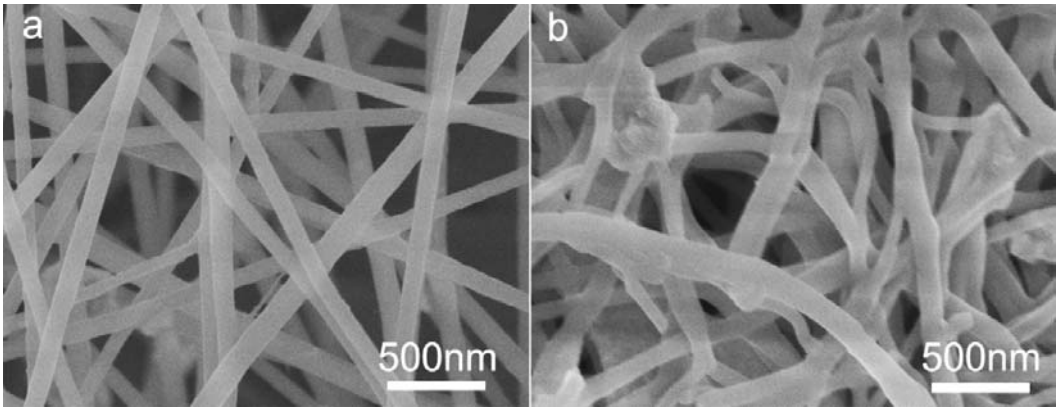

Fig. 1. Morphology of a) as-prepared membrane, b) oxidized membrane.

3.2. Optimization of the oxidation temperature(*T*), temperature gradient(*v*) and incubating time(*t*)

Oxidation temperature(*T*), temperature gradient(*v*) and incubating time(*t*) have effect on the photocatalytic property of Bismuth Tungstate/Acrylic Composite Nanofiber Membrane. Therefore, three parameters were evaluated by degradation rate of methylene blue. As shown in Fig. 2, with the increase of *T*, degradation rate of methylene blue increased at first followed by decreasing after 220°C. The oxidation temperature of 220°C showed the highest degradation rate, which could be contributed by the increase of the *T* promoting the formation of bismuth tungstate below 220°C

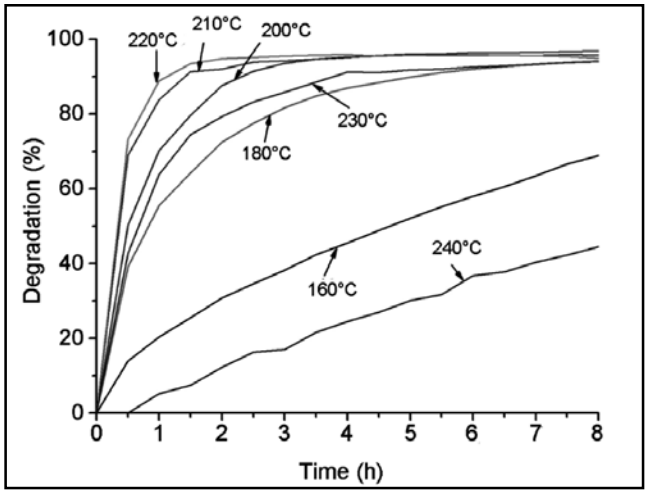

Fig. 2. The influence of oxidation temperature on methylene blue degradation.

and the decomposition of bismuth tungstate above 220°C. Obviously, the degradation rate of methylene blue at 220°C was the highest (95.53%) with better efficiency less than 4.5h (Fig. 2). For comparison, absorption of methylene blue of the sample at 220°C was tested in a dark room. Adsorption capacity was 16.7% after 4.5h, much lower than the degradation rate under light conditions, indicating that the membrane at 220°C has good visible light catalytic property.

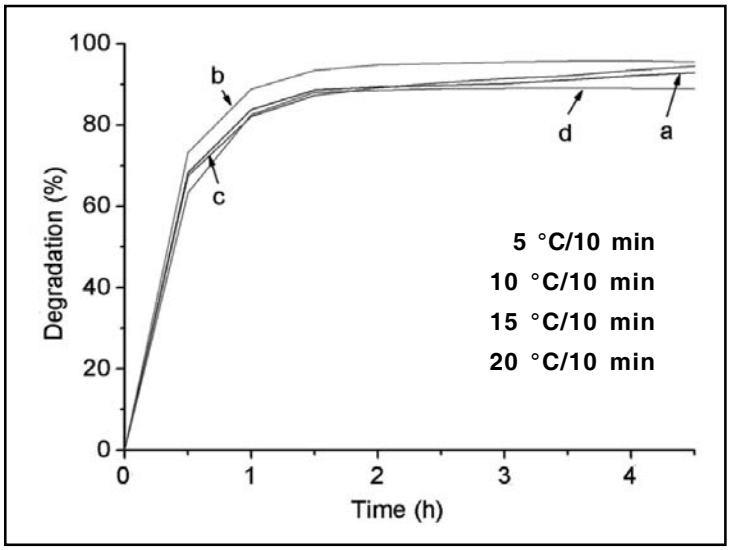

Fig. 3. The influence of temp gradient on methylene blue degradation.

To study the influence of temp gradient on methylene blue degradation, the as-prepared nanofiber membrane was heated from 40°C to 220°C at a certain rate (*V*) and incubated for the same time. Then the degradation rate of methylene blue was carried out for 4.5h. As shown in Fig. 3, with the increase of temperature gradient, the degradation rate increased firstly and decreased afterwards. This could be resulting from the fact that the temperature gradient can affect the reaction between the sodium nitrate and bismuth tungstate. The formation rate of bismuth tungstate was higher than the decomposition rate of bismuth tungstate under lower temperature gradient, while the decomposition rate was higher under higher temperature gradient [20]. It can be seen in Fig. 3 that the degradation rate was the highest at the temperature gradient of 10°C/10 min.

The incubated time can affect the resulting membrane property. In the study process, the as-prepared membrane was heated from 40°C to 220°C, at the rate of 10°C/10 min and incubated for some time (*t*). As shown in Fig. 4, with the increase of incubated time, the degradation rate increased at first and then

decreased. When the *t* more than 12h, the photocatalytic property of resulting membrane improved insignificantly. It can be speculated that the bismuth tungstate does not completely react under a critical incubated time, and above which bismuth tungstate does not increase any more. When the incubated time is 12h, the degradation rate was highest (Fig. 4).

It can be concluded that the bismuth tungstate/PAN composite nanofiber membrane achieved the best photocatalysis under the condition of *T*=220°C, *v*=10°C/10 min, *t*=12h.

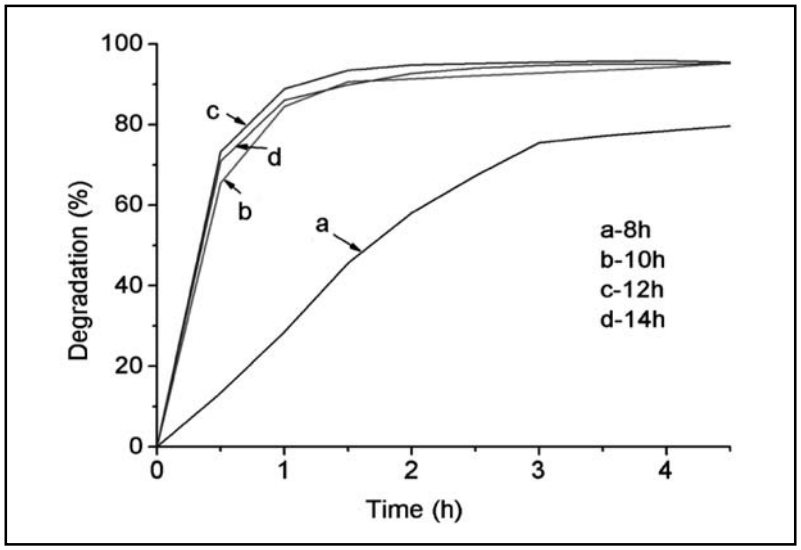

Fig. 4. The influence of incubated time on degradation rate of methylene blue

3.3. The structure characterization of resulting membrane at the condition of T=220°C, v=10°C/10 min, t=12h.

The membrane photocatalytic property is closely related to the internal membrane structure. To reveal the reason of the best photocatalytic property at the condition of T=220°C, v=10°C/10 min, t=12h, the as-prepared and oxidized membrane was characterized by FTIR. Compared with as-prepared membrane (Fig. 5a), the tendency of decreased peaks on 2242cm^{-1} (nitrile group), 2934cm^{-1} (vibrational contraction of methylene) indicated that the content decrease of nitrile group and chain structure in nanofiber. Meanwhile, the appearance of the peak on 1592 cm^{-1} (conjugate peak) suggested the cyclization of macromolecules and the trapezoidal structure change on molecular chains [21,22]. For the oxidized membrane (Fig. 5b), the appearance of the peak on 565cm^{-1} (W=O stretching vibration), 874 cm^{-1} (W-O asymmetrical stretching vibration), 994 cm^{-1} (W-O-W flexural vibration), suggesting the formation of bismuth tungstate after oxidation process [21].

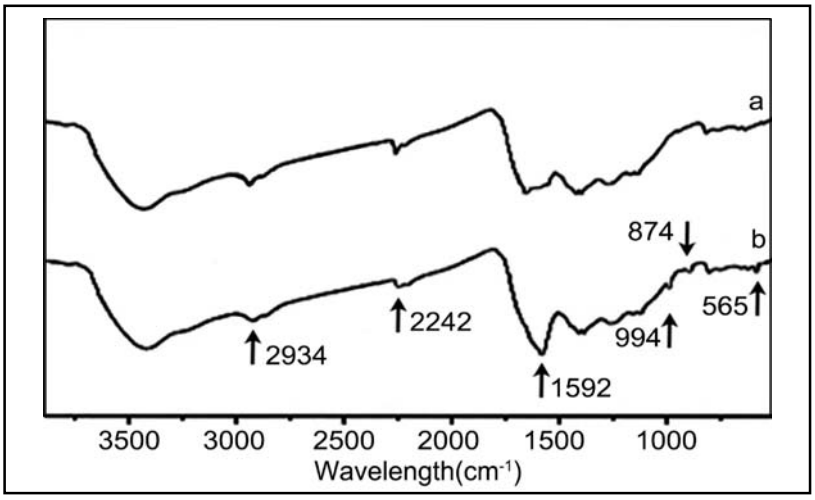

Fig. 5. FTIR patterns of a) as-prepared membrane, b) oxidized membrane.

To further reveal the structure at the condition of T=220°C, v=10°C/10 min, t=12h, the as-prepared and oxidized membrane was characterized by XRD. As shown in Fig. 6b, the characteristic peaks appeared at 33.1, 47.6, 54.8, 68.6, 75.6, 78.2 which are consistent with the bismuth tungstate standard card (JCPDS No.39-0256), indicating the formation of bismuth tungstate after oxidation treatment. When the treatment temperature is higher than 200 °C, the layered crystal peak of perovskite plate appears [23-26]. In addition, the sharp diffraction

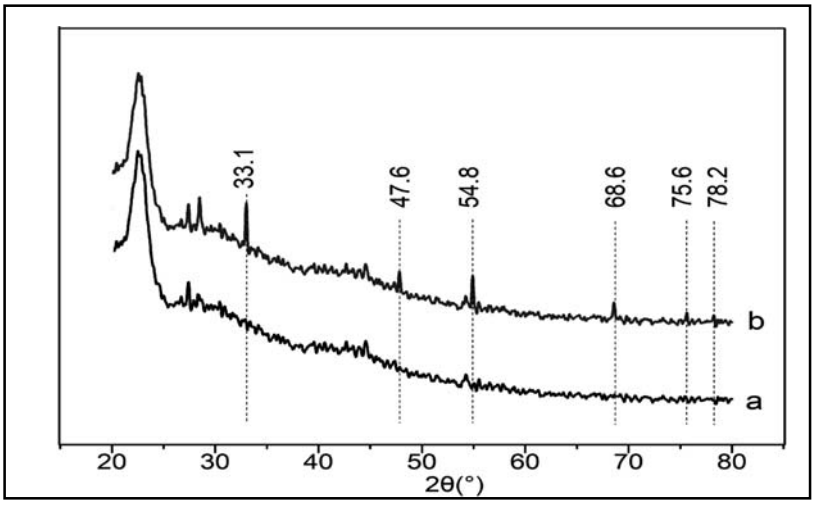

Fig. 6. XRD patterns of a) as-prepared membrane; b) oxidized membrane.

peaks illustrate the good crystallization of bismuth tungstate. Therefore, the good crystallization of bismuth tungstate with layered crystal endows the better photocatalytic property at the condition of T=220°C.

3.4. The membrane reusability of the methylene blue degradation

The photocatalysis reusability is an important indicator for practical application. Therefore, the reusability of bismuth tungstate/PAN composite nanofiber membrane was shown in

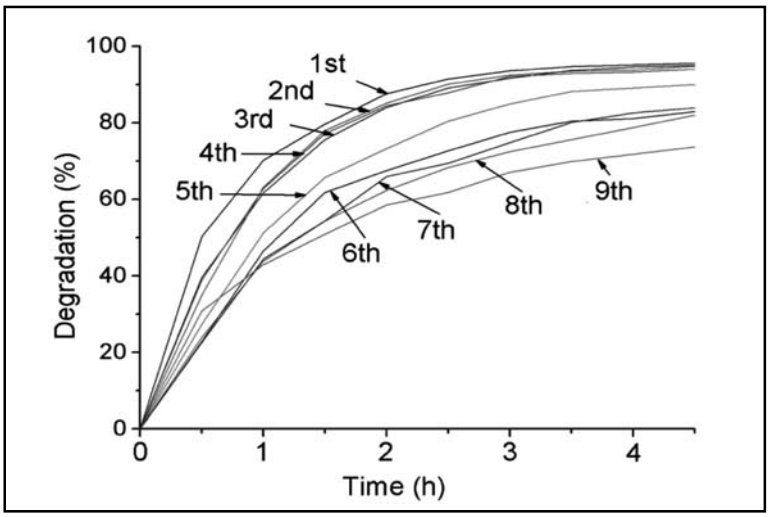

Fig. 7. The reusability of the bismuth tungstate/acrylic composite membrane

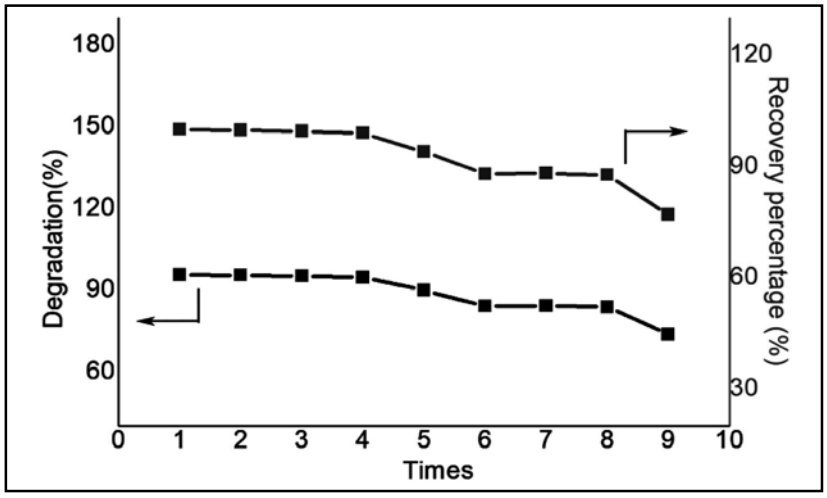

Fig. 8. The degradation and recovery percentage after several reuses.

Fig. 7 and Fig. 8. In the first reusable process, the degradation rate can retain 97.3% (Fig. 7). For the 2nd, 3rd and 4th reusable process, the catalytic activity can preserve the recovery percentage higher than 90%. (Fig. 8). For the fifth reuse process, the degradation rate decreased to 89.97%. The degradation rate of methylene blue still preserved 83.88% after reuse with eight times, indicating the bismuth tungstate/PAN composite nanofiber membrane possessing good photocatalytic property and reusability.

4. CONCLUSIONS

After parameter optimization, the electrospun bismuth tungstate/PAN composite nanofiber membrane achieved the highest photocatalytic property under Oxidation condition of T=220°C, v=10°C/10 min and t=12h. The photodegradation rate of methylene blue reached to 95.53% under optimized conditions. The good crystallization of bismuth tungstate with layered crystal favors to the excellent photocatalytic property. More importantly, the photodegradation rate of methylene blue still preserved 83.88% after 8 times reuse, suggesting its reusability. The outstanding photocatalytic property accompany with good reusability makes the resulting membrane as a good candidate for the water treatment.

Acknowledgement

This work was financially supported by the Natural Science Foundation of China (NO.21302001), Anhui Province Major Special Projects (NO.16030701088) and Talent start-up foundation of Anhui Polytechnic University (2017YQQ012).

REFERENCES

1. J Marugán, D Bru, C Pablos, M Catalá. *J. Hazard Mater*. 2012;213:117-122.
2. A Umar, MS Akhtar, A Al-Hajry, MS Al-Assiri, GN Dar, MS Islam*. Chem. Eng. J*. 2015;262:588-596.
3. N Zhang, R Ciriminna, M Pagliaro, Y J. Xu *Chem. Soc. Rev*. 2014;43(15):5276-5287.
4. M Qamar, A Khan. *Rsc Adv*. 2014;4(19):9542-9550.
5. M Chen, W Chu. *Appl. Catal. B-Environ*. 2015;169:175-182.
6. A Kudo, S Hijii. *Chem. Lett.* 1999;8(10):1103-1104.
7. XJ Dai, YS Luo, WD Zhang. SY. Fu *Dalton T.* 2010;39(14):3426-3432.
8. XH Zhang. *Indian J. Chem. A* 2017;56a:1028-1033.
9. C Xu, X Wei, Z Ren, Y, Wang, G Xu, G Shen, G Han. *Mater. Lett.* 2009;63(26):2194-2197.
10. H Hori, T Mai, T Mai, B Ohtani. *Catal. Today* 2018;300:99-111.
11. FE Ahmed, BS Lalia, R Hashaikeh. *Desalination* 2015;356:15-30.
12. CL Zhang, SH Yu. *Chem. Soc. Rev*. 2014;43(13):4423-4448.
13. Y Guibo, Z Qing, Z Yahong, Y Yin, Y Yumin. *J. Appl. Polym. Sci.* 2013;128(2):1061-1069.
14. D Kai, SS Liow, XJ Loh. *Mater. Sci. Eng. C* 2014;45:659-670.
15. W Xu, Y Feng, Y Ding, S Jiang, H Fang, H Hou. *Mater. Lett.* 2015;161:431-434.
16. S An, BN Joshi, MW Lee, NY Kim, SS Yoon. *Appl. Sur. Sci*. 2014;294:24-28.
17. X Liu, H Li, Q Tian, X Wu, Y Wang. *New Chem. Mater*. 2013;41(10):110-111.

18. HA Ahsaine, AE Jaouhari, A Slassi, M Ezahri, A Benlhachemi, B Bakiz, F Guinneton, JR Gavarri. *RSC Adv*. 2016;6(103):101105-101114.

19. M Ratova, R Marcelino, PD Souza, C Amorim, P Kelly. *Catalysts* 2017;7(10):283.

20. Y Liu, H Tang, H Lv, Z Ding, S Li. *Ceram. Int*. 2014;40(4):6203-6209.

21. G Shan, Y Fu, X Chu, C Chang, L Zhu. *J. colloid interf. Sci*. 2015;444:123-131.

22. M Ratova, RB Marcelino, PP Souza, CC Amorim, PJ Kelly. *Catalysts* 2017; 7(10):283.

23. TS Sian, GB Reddy. *Appl. Sur. Sci*. 2011;257:1972-1978.

24. J Huang, G Tan, A Xia, H Ren, L Zhang. *Res. Chem. Intermediat*. 2014; 40(2):903-911.

25. M Ratova, GT West, PJ Kelly. *Vacuum* 2015;115:66-69.

26. J Yang, X Shen, Y Li, L Bian, J Dai, D Yuan. *Chemcatchem* 2016; 8(7):1399-1409.

Received: 21-07-2017

Accepted: 24-08-2018